Structural Diversity in Thallium Chemistry

Part V[1])

Bromothallate(III) Salts of Mono- and Disubstituted Pyridinium Cations

by **Anthony Linden***[a]), **Alexander Petridis**[b]), and **Bruce D. James***[b])

[a]) Institute of Organic Chemistry, University of Zürich, Winterthurerstrasse 190, CH-8057 Zürich, Switzerland

[b]) Department of Chemistry, La Trobe University, Vic. 3086, Australia

From thallium(III) bromide solution, the unsubstituted pyridinium cation yields a complex (**1**) with the $[Tl_2Br_9]^{3-}$ anionic stoichiometry. The *Raman* spectrum and single-crystal X-ray crystallographic analysis showed that the salt contains independent $[TlBr_4]^-$ and bromide anions. A variety of mono- and disubstituted pyridinium cations were also employed in similar syntheses. The 2-bromopyridinium cation gave a salt **2** with $[TlBr_5]^{2-}$ stoichiometry, but the crystal structure revealed very weakly interacting $[TlBr_4]^-$ and bromide anions with a Tl ··· Br^- distance of 4.1545(6) Å. The 2-(ammoniomethyl)pyridinium and 2-amino-4-methylpyridinium cations yielded complexes containing $[TlBr_5]^{2-}$ (**3**) and $[TlBr_4]^-$ (**4**) species, respectively, which were confirmed by *Raman* spectroscopy and X-ray crystallographic analyses. For **3**, the $[TlBr_5]^{2-}$ anion has a highly distorted trigonal bipyramidal conformation with one long axial Tl ··· Br bond of 3.400(2) Å. Microanalytical results in conjunction with *Raman* spectra from a further five salts confirmed that they all contain the simple $[TlBr_4]^-$ anion. N–H ··· Br Hydrogen bonds clearly influence the nature of the anionic species obtained in these systems.

1. Introduction. – We are interested in the structural and possible stoichiometric diversity that may well be displayed by bromothallate(III) anions in their salts with simple organoammonium cations. Whilst a rich diversity among chlorothallate(III) anions has previously been established [2–9], less has been known with reference to bromothallate(III) anions, with most examples generally being limited to the $[TlBr_4]^-$ ion, and, to a lesser degree, the $[TlBr_6]^{3-}$ ion [2]. Our recent efforts, however, have expanded this horizon, and, so far, we have reported the isolation of bromothallate(III) salts containing such diverse species as discrete $[TlBr_5]^{2-}$ anions in both regular [1][10] and highly distorted, axially stretched trigonal bipyramidal forms [11], *cis*-bromo-bridged chains composed of $[TlBr_5]^{2-}$ units such that the Tl-atom is hexacoordinate [1], and mixed salts containing various combinations of unassociated anionic moieties like $[TlBr_4]^- + Br^-$ [1][11], $[TlBr_4]^- + [TlBr_6]^{3-}$ [1][10], and $[TlBr_4]^- + [TlBr_6]^{3-} + 4\ Br^-$ [1].

Halo-bridged confacial bioctahedral $[M_2X_9]^{3-}$ anions are well-known in certain main-group and transition-metal compounds, such as in the Cs salts containing $[Bi_2I_9]^{3-}$, $[Ti_2Cl_9]^{3-}$ or $[Mo_2Br_9]^{3-}$ [12], and $[Fe_2Cl_9]^{3-}$ [13]. A similar system has also been observed in the chlorothallate(III), $[Tl_2Cl_9]^{3-}$, and was one of the earliest examples studied by X-ray crystallography [2][12]. Also, dimerization of a $[TlCl_5]^{2-}$

[1]) For Part IV, see [1].

unit to give the discrete doubly-bridged $[Tl_2Cl_{10}]^{4-}$ anion occurs in the piperazinium [3] and hydrated calcium salts [14], as well as in combination with discrete $[TlCl_4]^-$ anions in the pyridinium salt [6]. Infinite *cis*-chloro-bridged chains occur with $[TlCl_5]^{2-}$ stoichiometry in the *p*-toluidinium and pentanediammonium salts and with $[Tl_2Cl_{10}]^{4-}$ stoichiometry in the adamantane-2-ammonium salt [3].

For the corresponding bromothallate(III) systems, evidence of halo-bridging in the solid state has been observed only in the room-temperature α-phase of $Cs_3Tl_2Br_9$ [15] and in the *N*-methylpropane-1,3-diammonium pentabromothallate(III) salt [1], both of which contain, among other species, *cis*-bromo-bridged $[TlBr_5]^{2-}$ chains made up of corner-shared $[TlBr_6]^{3-}$ octahedra. As a continuation of our investigations, we began using a range of mono- and disubstituted pyridinium cations on the basis that both the chloro- and the bromothallate(III) salts acquired with the unsubstituted pyridinium cation were found to possess the $[Tl_2X_9]^{3-}$ stoichiometry, although in neither case was a discrete binuclear $[Tl_2X_9]^{3-}$ unit obtained. The range of ring substituents available in pyridinium systems provides an opportunity to explore possible relationships between a cation's H-bonding ability (N–H ··· Br) and its pK_a value. Furthermore, we wished to ascertain whether any structural relationships existed between the known chlorothallate(III) complexes that display halo-bridging and their bromothallate(III) counterparts. We now report the results of these investigations, and the cations chosen for this work are listed in *Table 1*.

2. Experimental. – 2.1. *Syntheses.* All reagents were obtained from *Aldrich*, Milwaukee, WI, and used as received. High yields of thallium(I) bromide were obtained *via* the reaction of thallium(I) nitrate or sulfate and dil. HBr, according to the method described by *Brauer* [17]. Freshly prepared thallium(I) bromide was suspended in the appropriate solvent (*Table 1*) and oxidized by warming with a slight excess of dibromine [17]. The bromothallate(III) complexes **1**–**9** were conveniently prepared, as described previously [1][10][11], by adding an equimolar quantity of organic base to the $TlBr_3$ in the chosen solvent and then warming the mixture to dissolve any resulting precipitate. For crystal growth, various evaporation techniques were employed to minimize the rate of vapor diffusion and solvent loss so that well-formed crystals could be obtained. None of the complexes appeared to be particularly moisture-sensitive, but were stored routinely in a desiccator over P_2O_5 and KOH.

It is known that the nature of the compounds obtained from aq. soln. is determined by complicated heterogeneous equilibrium, and perhaps kinetic factors, with these depending *inter alia* upon cation size [2]. In the case of complex **1**, it was found that variation of the cation/Tl ratio between 1:1 and 3:1 had no effect on the nature of the product that crystallized from soln., a material with the stoichiometry $(cation)_3 \cdot Tl_2Br_9$ being formed in every case (and this paralleled the chlorothallate(III) system [6]). To make direct comparisons and to retain reasonably consistent synthetic conditions, the 1:1 cation/Tl stoichiometric ratio was also employed for each of the other cations listed.

2.2. Raman *Spectroscopy. Raman* spectra were recorded by means of a *Renishaw Ramanscope* model *2000* with 633- or 780-nm laser excitation. The spectra obtained on this instrument yielded only the stretching frequencies in the range of 150–250 cm^{-1} (the bending frequencies for bromothallate(III) complexes occur below 100 cm^{-1}, which is outside the range of the instrument).

2.3. *X-Ray Crystallography.* The crystallographic data for complexes **1**–**4** are given in *Table 2*[2]). All measurements were conducted at low-temp. with graphite-monochromated MoK_α radiation ($\lambda = 0.71073$ Å). A *Rigaku AFC5R* diffractometer and a 12-kW rotating anode generator was used for **3**, while a *Nonius KappaCCD* diffractometer was used for **1**, **2**, and **4**. No crystal decay was detected. The intensities were

---

[2]) CCDC-180294, 186239, 180295, and 180296 contain the supplementary crystallographic data for complexes **1**–**4**, resp. These data can be obtained, free of charge, *via* www.ccdc.cam.ac.uk/conts/retrieving.html (or from the Cambridge Crystallographic Data Centre, 12 Union Road, Cambridge CB21EZ, UK (fax: + 44 1223 336033; e-mail: deposit@ccdc.cam.ac.uk)).

Table 1. *Preparative Data for the Bromothallate(III) Complexes*

	Organic cation	Cation pK_a [a])	Solvent	Crystal color/form	Crop	M.p. [°]	Microanalysis [b]) [c]) [%]	Formula
1	Pyridinium	5.25	MeOH	yellow prism	1st	141	Found: C 13.22, H 1.28, Br 51.98, N 3.13 Calc.: C 13.16, H 1.32, Br 52.55, N 3.07	$[C_5H_6N]_3 \cdot [TlBr_4]_2 \cdot Br$
2	2-Bromopyridinium	0.9	conc. HBr	yellow-orange plates	1st	130	Found: C 13.07, H 0.95, Br 60.72, N 3.36 Calc.: C 13.02, H 1.09, Br 60.67, N 3.04	$[C_5H_5BrN]_2 \cdot [TlBr_4] \cdot Br$
3	2-(Ammoniomethyl)-pyridinium	8.78	MeCN	yellow irregular prisms	1st	155	Found: C 10.15, H 1.21, Br 55.7, N 3.86 Calc.: C 10.09, H 1.14, Br 55.94, N 3.92	$[C_6H_{10}N_2] \cdot [TlBr_5]$
4	2-Amino-4-methyl-pyridinium	7.48	conc. HBr	yellow-orange prisms	2nd	130	Found: C 11.44, H 1.34, Br 50.94, N 4.74 Calc.: C 11.38, H 1.43, Br 50.47, N 4.42	$[C_6H_9N_2] \cdot [TlBr_4]$
5	2-Amino-3-methyl-pyridinium	7.24	conc. HBr	yellow-orange prisms	1st	163	Found: C 10.92, H 1.21, Br 49.98, N 4.34 Calc.: C 11.38, H 1.43, Br 50.47, N 4.42	$[C_6H_9N_2] \cdot [TlBr_4]$
6	4-Methylpyridinium	6.03	conc. HBr	orange prisms	1st	150	Found: C 11.71, H 1.16, Br 51.64, N 2.21 Calc.: C 11.66, H 1.30, Br 51.71, N 2.26	$[C_6H_8N] \cdot [TlBr_4]$
7	2,6-Dimethyl-pyridinium	6.6	conc. HBr	orange prisms	1st	136	Found: C 13.36, H 1.50, Br 49.91, N 2.43 Calc.: C 13.29, H 1.59, Br 50.50, N 2.22	$[C_7H_{10}N] \cdot [TlBr_4]$
8	2-Aminopyridinium	8.71	conc. HBr	orange prisms	1st	113	Found: C 9.71, H 1.07, Br 50.62, N 4.78 Calc.: C 9.69, H 1.14, Br 51.62, N 4.52	$[C_5H_7N_2] \cdot [TlBr_4]$
9	4-(Dimethylamino)-pyridinium	9.7	conc. HBr	yellow prisms	1st	190	Found: C 12.96, H 1.64, Br 49.58, N 4.24 Calc.: C 12.99, H 1.71, Br 49.39, N 4.33	$[C_7H_{11}N_2] \cdot [TlBr_4]$

[a]) The pK_a values are taken from [16]. [b]) Microanalyses were performed by the *Campbell Microanalytical Laboratory*, University of Otago, New Zealand. [c]) The calculated values are based on the formula shown.

corrected for *Lorentz* and polarization effects. A numerical absorption [18] was applied to the data for **1** and **2**, while an analytical absorption correction [19] was applied for **3**. An absorption correction by means of SORTAV, which is based on an analysis of symmetry-equivalent reflections in the highly redundant data set [20], was applied in the case of **4**. Each structure was solved by direct methods with SIR92 [21]. This revealed, at a minimum, the positions of the Tl- and Br-atoms, and all remaining non-H-atoms were located in subsequent difference *Fourier* maps.

For **1**, similarity restraints were applied to the bond lengths and angles within the three chemically equivalent, but symmetry-independent cations. As the rings of the cations in **1**, **2**, and **3** have a certain degree of symmetry, and N^+ is isoelectronic with the C-atom, there is potential uncertainty in deciding which of the ring atoms is the N-atom. The N-atoms were initially assigned by calculating a difference *Fourier* map phased on only the Tl- and Br-atoms, and selecting the peak in each ring that was the uppermost in the peak list. Examining all H ··· Br distances between the rings and the Br-atoms subsequently vindicated this procedure. The shortest and most linear contacts were always those involving the H-atoms bonded to the N-atoms, and only these distances were consistent with H-bonding interactions.

The non-H-atoms were refined anisotropically, while all of the H-atoms were placed in geometrically calculated positions and refined with a riding model in which each H-atom was assigned a fixed isotropic displacement parameter with a value equal to $1.2U_{eq}$ of its parent atom ($1.5U_{eq}$ for CH_3 and NH_3^+ groups). A circular *Fourier* map was calculated and used to estimate the orientation of the NH_3^+ group in **3**. In adding the H-atoms to the model for **4**, it was assumed that the cation is protonated at the pyridine N-atom. This assumption was supported by the knowledge that logical N–H ··· Br H-bonds are evident when this N-atom is protonated.

Refinement of each structure was carried out on F^2 with full-matrix least-squares procedures, which minimized the function $\Sigma w(F_o^2 - F_c^2)^2$. Corrections for secondary extinction were applied, except in the case of **4**. For **2** and **3**, two and eleven reflections, respectively, whose intensities were considered to be outliers, were omitted from the final cycles of refinement. For each structure, the largest peaks of residual electron density were always within the vicinity of the Tl- or Br-atoms.

Scattering factors for non-H-atoms were taken from [22], and the scattering factors for H-atoms were taken from [23]. The values of the mass attenuation coefficients were those of [24]. All calculations were performed with SHELXL97 [25]. The figures were drawn with ORTEPIII [26] and the PLUTON routine in the program PLATON [27].

3. Results and Discussion. – 3.1. *Tris(pyridinium)bis[tetrabromothallate(III)] Bromide* (**1**). The unsubstituted pyridinium cation resulted in the formation of a bromothallate(III) complex with the $[Tl_2Br_9]^{3-}$ anionic stoichiometry (**1**). The X-ray crystallographic analysis revealed that the dimeric $[Tl_2Br_9]^{3-}$ species was not present. Instead, the asymmetric unit contains three symmetry-independent pyridinium cations, two $[TlBr_4]^-$ anions and a Br^- ion (*Fig. 1*). The Br^- ion, Br(9), is positioned between the two $[TlBr_4]^-$ anions with a Tl(1) ··· Br(9) ··· Tl(2) angle of 116.86(2)° and is virtually *trans* to Br(1) in one $[TlBr_4]^-$ anion and Br(8) in the other (*Table 3*). This looks like a *pseudo*-$[Tl_2Br_9]^{3-}$ grouping, but the Br^- ion is 4.6370(8) and 4.5204(9) Å from Tl(1) and Tl(2), respectively. These distances are greater than the sum (*ca.* 4.3 Å [28]) of the *Van der Waals* radii of the atoms involved, so that the Br^- ion is not interacting significantly with the Tl-atoms. This is supported by minimal distortions of the $[TlBr_4]^-$ anions from ideal tetrahedral geometry. The lone Br^- ion is the sole acceptor of H-bonds in the structure (*Table 4*). It accepts one H-bond from each symmetry-independent cation, which essentially produces a dipositive tetrameric grouping (*Fig. 1*). The H-bonding interactions do not link the ions into extended networks or chains.

Although the system in **1** comes close to adopting a $[Tl_2Br_9]^{3-}$ anionic structure, it must be described as being composed of discrete $[TlBr_4]^-$ and Br^- ions. Conceivably, certain molecular parameters such as the size, shape, charge, and basicity of the pyridinium cation might influence packing considerations, and, hence, prevent the

Table 2. *Crystallographic Data for* $[C_5H_6N]_3\cdot[TlBr_4]_2\cdot Br$ (**1**), $[C_5H_5BrN]_2\cdot[TlBr_4]\cdot Br$ (**2**), $[C_6H_{10}N_2]\cdot[TlBr_5]$ (**3**), *and* $[C_6H_9N_2]\cdot[TlBr_4]$ (**4**)

	1	**2**	**3**	**4**
Crystallized from	MeOH	conc. HBr	MeCN	conc. HBr
Empirical formula	$C_{15}H_{18}Br_9N_3Tl_2$	$C_{10}H_{10}Br_7N_2Tl$	$C_6H_{10}Br_5N_2Tl$	$C_6H_9Br_4N_2Tl$
Formula weight [g mol^{-1}]	1368.1	921.83	713.98	633.07
Crystal color, habit	pale yellow, prism	yellow-orange, plate	pale yellow, tablet	yellow-orange, prism
Crystal dimensions [mm]	$0.15\times0.30\times0.30$	$0.05\times0.12\times0.20$	$0.09\times0.27\times0.46$	$0.15\times0.22\times0.30$
Temp. [K]	160(1)	160(1)	173(1)	160(1)
Crystal system	orthorhombic	triclinic	monoclinic	orthorhombic
Space group	*Pbca*	$P\bar{1}$	$P2_1/n$	*Pbca*
Z	8	2	4	8
Reflections for cell determination	153662	31483	25	76658
2θ Range for cell [°]	4 – 60	4 – 60	36 – 40	4 – 60
a [Å]	13.4041(1)	6.4981(1)	10.212(2)	9.1648(1)
b [Å]	16.3145(1)	10.8301(1)	6.912(2)	15.0095(1)
c [Å]	27.6173(2)	15.5014(2)	20.621(3)	19.8468(2)
α [°]	90	72.9756(5)	90	90
β [°]	90	86.9797(5)	97.03(2)	90
γ [°]	90	73.7306(6)	90	90
V [Å^3]	6039.38(7)	1000.83(2)	1444.6(4)	2730.11(4)
$F(000)$	4848	820	1264	2240
D_x [g cm^{-3}]	3.009	3.059	3.368	3.080
$\mu(\mathrm{Mo}K_\alpha)$ [mm^{-1}]	22.59	22.061	25.00	23.52
Transmission factors [min; max]	0.013; 0.115	0.049; 0.253	0.013; 0.124	0.006; 0.081
Scan type	ϕ and ω	ϕ and ω	$\omega/2\theta$	ϕ and ω
$2\theta_{max}$ [°]	60	60	60	60
Reflections measured	134487	44210	4766	69788
Symmetry-independent reflections	8794	5829	4213	3984
R_{int}	0.225	0.099	0.067	0.163
Reflections with $I>2\sigma(I)$	6087	5160	2594	3078
Parameters refined	263 (72 restraints)	182	129	120
R (on F; $I>2\sigma(I)$ reflections)	0.0430	0.0303	0.0604	0.0442
wR (on F^2; all indept. reflections)	0.1067	0.0757	0.1668	0.1161
Weighting parameters [a; b] [a])	0.0388; 11.0316	0.0352; 1.4255	0.0881; 0.0	0.0512; 12.3327
Goodness-of-fit	1.024	1.058	1.009	1.035
Secondary extinction coeff.	0.00014(2)	0.0031(2)	0.0006(2)	0
Final Δ_{max}/σ	0.002	0.002	0.001	0.002
$\Delta\rho$(max; min) [e Å^{-3}]	1.79; −2.72	1.25; −2.12	2.67; −3.63	2.30; −1.84

[a]) $w^{-1}=\sigma^2(F_o^2)+(aP)^2+bP$ where $P=(F_o^2+2F_c^2)/3$

Table 3. *Selected Interatomic Distances* [Å] *and Angles* [°] *for* $[C_5H_6N]_3 \cdot [TlBr_4]_2 \cdot Br$ (**1**), $[C_5H_5BrN]_2 \cdot [TlBr_4] \cdot Br$ (**2**), $[C_6H_{10}N_2] \cdot [TlBr_5]$ (**3**), *and* $[C_6H_9N_2] \cdot [TlBr_4]$ (**4**), *with Standard Uncertainties in Parentheses*

Complex **1**			
Tl(1)–Br(1)	2.5638(8)	Tl(2)–Br(5)	2.5420(7)
Tl(1)–Br(2)	2.5328(8)	Tl(2)–Br(6)	2.5505(7)
Tl(1)–Br(3)	2.5659(8)	Tl(2)–Br(7)	2.5723(8)
Tl(1)–Br(4)	2.5596(8)	Tl(2)–Br(8)	2.5596(9)
Tl(1) ··· Br(9)	4.6370(8)	Tl(2) ··· Br(9)	4.5204(9)
Br(1)–Tl(1)–Br(2)	112.08(3)	Br(5)–Tl(2)–Br(6)	113.80(3)
Br(1)–Tl(1)–Br(3)	110.68(3)	Br(5)–Tl(2)–Br(7)	109.57(3)
Br(1)–Tl(1)–Br(4)	105.67(3)	Br(5)–Tl(2)–Br(8)	112.15(3)
Br(2)–Tl(1)–Br(3)	107.00(3)	Br(6)–Tl(2)–Br(7)	109.15(3)
Br(2)–Tl(1)–Br(4)	114.08(3)	Br(6)–Tl(2)–Br(8)	107.47(3)
Br(3)–Tl(1)–Br(4)	107.26(3)	Br(7)–Tl(2)–Br(8)	104.22(3)
Br(1)–Tl(1) ··· Br(9)	175.63(2)	Br(8)–Tl(2) ··· Br(9)	171.87(3)
Complex **2**			
Tl–Br(1)	2.5686(4)	Tl–Br(4)	2.5392(4)
Tl–Br(2)	2.5357(4)	Tl ··· Br(5)	4.1545(6)
Tl–Br(3)	2.5805(5)		
Br(1)–Tl–Br(2)	106.98(2)	Br(2)–Tl–Br(4)	125.65(2)
Br(1)–Tl–Br(3)	108.13(2)	Br(3)–Tl–Br(4)	104.52(2)
Br(1)–Tl–Br(4)	106.36(2)	Br(3)–Tl ··· Br(5)	164.32(1)
Br(2)–Tl–Br(3)	104.25(2)		
Complex **3**			
Tl–Br(1)	3.400(2)	Tl–Br(4)	2.570(2)
Tl–Br(2)	2.606(2)	Tl–Br(5)	2.548(1)
Tl–Br(3)	2.570(2)		
Br(1)–Tl–Br(2)	174.43(4)	Br(2)–Tl–Br(4)	99.18(5)
Br(1)–Tl–Br(3)	79.42(4)	Br(2)–Tl–Br(5)	107.83(5)
Br(1)–Tl–Br(4)	79.92(4)	Br(3)–Tl–Br(4)	121.25(5)
Br(1)–Tl–Br(5)	77.48(4)	Br(3)–Tl–Br(5)	115.27(5)
Br(2)–Tl–Br(3)	96.52(5)	Br(4)–Tl–Br(5)	112.74(5)
Complex **4**			
Tl–Br(1)	2.5691(8)	Tl–Br(3)	2.5568(9)
Tl–Br(2)	2.5463(8)	Tl–Br(4)	2.5427(9)
Br(1)–Tl–Br(2)	111.78(3)	Br(2)–Tl–Br(3)	110.92(3)
Br(1)–Tl–Br(3)	108.06(3)	Br(2)–Tl–Br(4)	107.66(3)
Br(1)–Tl–Br(4)	107.04(3)	Br(3)–Tl–Br(4)	111.35(4)

contraction of the *pseudo*-$[Tl_2Br_9]^{3-}$ grouping to a true one. On the other hand, the ability of the cation to form N–H ··· Br H-bonds is evidently exerting a considerable influence on the overall system, and could also play a role in determining the nature of the anionic grouping observed in complex **1**. The inhibitory effect of cations with H-bond-donor capabilities on the ability of $[TlBr_4]^-$ and Br^- ions to condense into $[TlBr_5]^{2-}$ anions in similar systems has been discussed recently [1].

The structure of complex **1** is rather akin to that of the 4-chloropyridinium ([4-Cl(py)H]$^+$) salt of the chloroferrate(III). This salt has the $[4\text{-Cl(py)H}]_3Fe_2Cl_9$ stoichiometry, but was shown by X-ray crystallography to contain two slightly distorted tetrahedral $[FeCl_4]^-$ anions, one Cl^- anion, and three [4-Cl(py)H]$^+$ cations in the asymmetric unit. In this material, all three cations were H-bonded to the single Cl^-

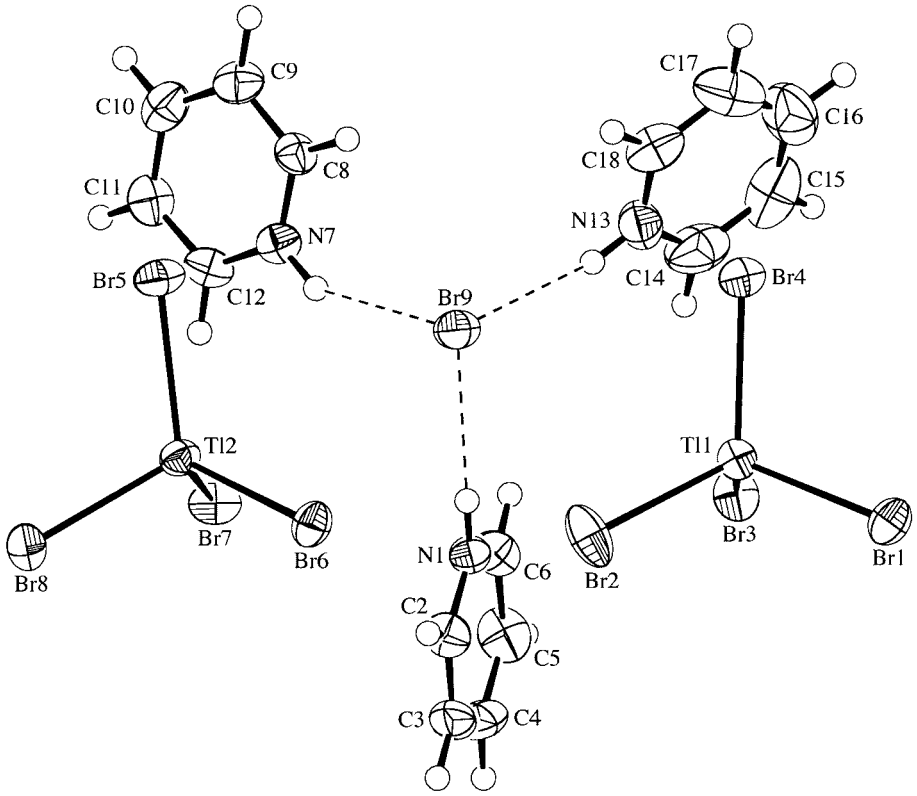

Fig. 1. *The asymmetric unit of the* $[C_5H_6N]_3 \cdot [TlBr_4]_2 \cdot Br$ (**1**) *salt showing the pseudo-*$[Tl_2Br_9]^{3-}$ *grouping and the H-bonding interactions between the cations and the lone bromide ion* (50% probability ellipsoids)

anion, just as in **1**. Replacement of the $[4\text{-Cl(py)H}]^+$ cation with the larger 4-bromopyridinium species yielded an isomorphous chloroferrate(III) material [29].

For $Cs_3Tl_2Br_9$, X-ray diffraction showed that the ambient temperature α-form was assembled from $[TlBr_6]^{3-}$ octahedra, linked into chains with $[TlBr_5]^{2-}$ stoichiometry by sharing vertices, plus isolated $[TlBr_4]^-$ tetrahedra [15]. Above 170°, the β-form shows no evidence for $[TlBr_4]^-$ species, but also no evidence for discrete $[Tl_2Br_9]^{3-}$ anions. As far as we know, no other $[Tl_2Br_9]^{3-}$ systems that would allow comparison of structural data have been discovered.

3.2. *Cation Influences on the Tl(III) Coordination Sphere.* A likely central component in rationalizing the failure of the anionic unit in **1** to form a dimeric $[Tl_2Br_9]^{3-}$ species appears to be the presence of H-bonding. This structure can be deemed to be the definitive extreme result of H-bonds 'pulling' a Br-atom away from a true $[TlBr_5]^{2-}$ or $[Tl_2Br_9]^{3-}$ anion so that it is finally situated in the position observed. This arrangement precludes any significant interaction with the $[TlBr_4]^-$ anions and any effect on the coordination geometry.

The H-bonding behavior in some substituted anilinium chloride and trichlorostannate(II) derivatives has been investigated by IR and XPS methods. These results

Table 4. *H-Bonding Parameters for the Bromothallate(III) Complexes* **1**–**4**

D–H ··· A [a])	D–H [Å]	H ··· A [Å]	D ··· A [Å]	D–H ··· A [°]
Complex **1**				
N(1)–H(1) ··· Br(9)	0.88	2.40	3.211(5)	153
N(7)–H(7) ··· Br(9)	0.88	2.48	3.259(6)	147
N(13)–H(13) ··· Br(9)	0.88	2.41	3.260(7)	162
Complex **2**				
N(1)–H(1) ··· Br(5)	0.88	2.33	3.198(4)	167
N(7)–H(7) ··· Br(5)	0.88	2.35	3.206(4)	165
Complex **3**				
N(1)–H(1) ··· Br(1^{i})	0.88	2.85	3.49(1)	131
N(1)–H(1) ··· Br(5^{i})	0.88	2.86	3.61(1)	145
N(2)–H(21) ··· Br(1^{ii})	0.91	2.52	3.32(1)	147
N(2)–H(21) ··· Br(4^{ii})	0.91	3.00	3.58(1)	123
N(2)–H(22) ··· Br(1^{i})	0.91	2.48	3.24(1)	140
N(2)–H(23) ··· Br(3)	0.91	2.59	3.50(1)	174
Complex **4**				
N(1)–H(1) ··· Br(1^{iii})	0.88	3.06	3.669(8)	128
N(1)–H(1) ··· Br(3^{iv})	0.88	2.82	3.572(8)	145
N(2)–H(2a) ··· Br(1^{iii})	0.88	2.95	3.558(9)	128
N(2)–H(2b) ··· Br(2^{v})	0.88	2.77	3.61(1)	159
N(2)–H(2a) ··· Br(4^{v})	0.88	2.81	3.439(9)	129

[a]) Symmetry operators: [i] $5/2 - x, y - 1/2, 3/2 - z$; [ii] $x, y - 1, z$; [iii] $x - 1, y, z$; [iv] $x - 1/2, y, 1/2 - z$; [v] $x - 1/2, 3/2 - y, - z$.

indicate that the degree of H-bonding depend on the position of substituents on the aniline aromatic ring and is correlated with the dissociation constants, pK_a [30]. Supplementary studies by MOPAC/AM1 investigated the activity of H-bonds through the estimation of atomic charge distributions in some N–H ··· Cl H-bonded anilinium derivatives. The theoretical results suggested that the substituents affect that part of the structure that includes N–H ··· Cl H-bonding and change the degree of H-bonding and partial charge residing on the N- and H-atoms [31].

Based on the above hypothesis, the N–H ··· Br H-bond in bromothallate(III) complexes is expected to be affected by the availability of the base lone pair, which, in turn, is related to the influence of any substituent groups on the pyridinium aromatic ring, and, so, correlates with their basicity, as reflected by their dissociation constants, pK_a. Therefore, if it is possible to modify the strength/effect of H-bonding in such complexes, this factor might influence the formation of an enneabromodithallate(III), $[Tl_2Br_9]^{3-}$, species at ambient temperature. Accordingly, a strategy was followed in which mono- and disubstituted pyridinium cations containing Me, NH_2, and Br substituents in varying orientations around the pyridinium ring were employed in syntheses. This provided a series of related cations with varying basicities (*Table 1*) that have the potential to influence the degree of N–H ··· Br H-bonding present in bromothallate(III) complexes and that also serve to alter the steric bulk of the pyridinium cation. It was hoped that these properties might influence the coordination sphere of Tl, as has been observed with some previously reported bromothallate(III)

complexes that have been found to exhibit a variety of coordination geometries, such as $[TlBr_4]^-$, $[TlBr_5]^{2-}$, and $[TlBr_6]^{3-}$ [1][10][11].

3.3. *Bis(2-bromopyridinium) Tetrabromothallate(III) Bromide* (**2**). Complex **2** analyses as $[C_5H_5BrN]_2 \cdot [TlBr_5]$ (*Table 1*). In the crystal structure, the asymmetric unit contains two symmetry-independent cations, one $[TlBr_4]^-$ anion and a Br^- ion with none of these entities occupying any special symmetry sites (*Fig. 2*). The arrangement of the ions in the structure is very similar to that in the pyridinium structure and can be thought of as being derived from the latter by removing one cation and one $[TlBr_4]^-$ anion. The Br^- ion, Br(5), lies 4.1545(6) Å from the Tl-atom, which is just inside the sum of the *Van der Waals* radii of these atoms, and the slight distortion of the tetrahedral geometry of the $[TlBr_4]^-$ anion is consistent with the existence of a very weak interaction between the $[TlBr_4]^-$ anion and the Br^- ion (*Table 3*). The Br^- ion is correctly positioned to be considered as forming the distant apex of a distorted $[TlBr_5]^{2-}$ trigonal bipyramid, as it is nearly *trans* to Br(3) with a Br(3)–Tl ··· Br(5) angle of 164.32(1)°, and the Tl–Br(3) bond is correspondingly marginally longer than the other three Tl–Br bonds. The Br(2)–Tl–Br(4) angle has opened significantly from the normal tetrahedral angle to 125.65(2)°, which may be due to the Br^- ion sitting closer into the 'V' created by Br(2)–Tl–Br(4) than being directly above the Br(1), Br(2), Br(4) triangle. This is supported by the Br–Tl–Br angles involving Br(3), which show that Br(2) and Br(4), but not Br(1), are being pushed slightly away from the Br^- ion towards Br(3). As with complex **1**, the Br^- ion is the sole acceptor of H-bonds in the structure (*Table 4*). It accepts one H-bond from each symmetry-independent cation to produce a positively charged trimeric grouping (*Fig. 2*). The H-bonding interactions do not link the ions into an extended network or chains.

We have described other complexes containing distorted $[TlBr_5]^{2-}$ species with very long Tl ··· Br contacts of up to *ca.* 3.77 Å (see [11] and *3.4* below), but complex **2** represents the longest known Tl ··· Br contact in which the distant Br^- ion appears to be influencing the coordination geometry of the Tl-atom. This implies that a Tl ··· Br distance of 4.15 Å is still slightly less than the sum of the *Van der Waals* radii of the Tl- and Br-atoms and lends further support to the reference values of these radii [28], whose sum is *ca.* 4.3 Å.

3.4. *2-(Ammoniomethyl)pyridinium Pentabromothallate(III)* (**3**). Complex **3** analyses as $[C_6H_{10}N_2] \cdot [TlBr_5]$ (*Table 1*). In the crystal structure, the asymmetric unit contains one cation and a highly distorted trigonal bipyramidal $[TlBr_5]^{2-}$ anion with one long axial Tl–Br bond of 3.400(2) Å (*Table 3* and *Fig. 3*). This geometry can effectively be described as being derived from the distortion of a tetrahedral $[TlBr_4]^-$ unit by the close approach of the fifth Br-atom. The Tl–Br bonds involving Br(3), Br(4) and Br(5), which would be equatorial in a symmetrical trigonal bipyramidal ion, are bent at the metal atom away from Br(2) towards the more distant Br(1)-atom. The distances of Tl, Br(1), and Br(2) from the least-squares equatorial plane defined by Br(3), Br(4), and Br(5) are 0.4901(6), −2.908(1) and 3.077(1) Å, respectively. Thus, the two axial Br-atoms are almost equidistant from the equatorial plane, and all five Br-atoms clearly belong to the one trigonal bipyramidal anionic unit in which the Tl-atom is displaced significantly towards one of the axial Br-atoms. The Tl–Br(2) bond, which is *trans* to the long interaction, is only slightly longer than the equatorial Tl–Br bonds.

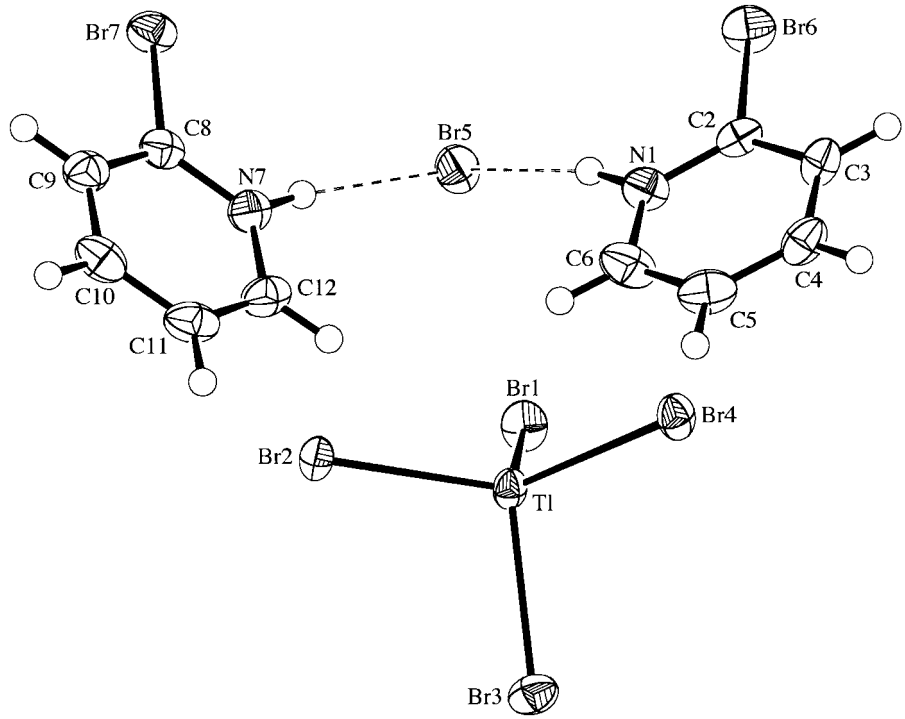

Fig. 2. *The asymmetric unit of the* $[C_5H_5BrN]_2 \cdot [TlBr_4] \cdot Br$ (**2**) *salt showing the pseudo-*$[TlBr_5]^{2-}$ *grouping and the H-bonding interactions between the cations and the lone bromide ion* (50% probability ellipsoids)

The long axial Tl–Br distance in **3** is intermediate between the very long axial Tl ··· Br interactions (*ca.* 3.77 Å) found in the structures of the piperazinium and 2,2′-bipyridinium pentabromothallate(III) salts [11], and those in the more regular $[TlBr_5]^{2-}$ species found in the 1,1,4,4-tetramethylpiperazinium, *N*,*N*′-diethyltriethylenediammonium and *N*,*N*′-diethyl-*N*,*N*,*N*′,*N*′-tetramethylethylene-1,2-diammonium salts in which the longest axial Tl–Br bonds are in the range 2.73 to 2.92 Å [1][10][32]. Accordingly, the trigonal bipyramidal geometry of **3** is less distorted than in the structures displaying the very long Tl ··· Br interactions and the Br(1)-atom may be described as undergoing 'secondary' bonding [33] with the Tl-atom.

The H-atom on the pyridinium N-atom forms bifurcated H-bonds, one interaction being with the weakly bound axial Br-atom of the $[TlBr_5]^{2-}$ anion, and the other with one of the equatorial Br-atoms in the same anion (*Table 4*). The ammoniomethyl group forms four H-bonds with one of the three H-atoms being involved in bifurcated H-bonding. The weakly bound axial Br-atom accepts two of these interactions, while the other two interactions are with the two equatorial Br-atoms not otherwise involved (*Fig. 4*). The weakly bound axial Br-atom, therefore, accepts a total of three H-bonds from two different cations, and each equatorial Br-atom accepts one interaction, each coming from a different cation, one of which is also donating the two interactions from the pyridinium N-atom. The more strongly bound axial Br-atom is not involved in any

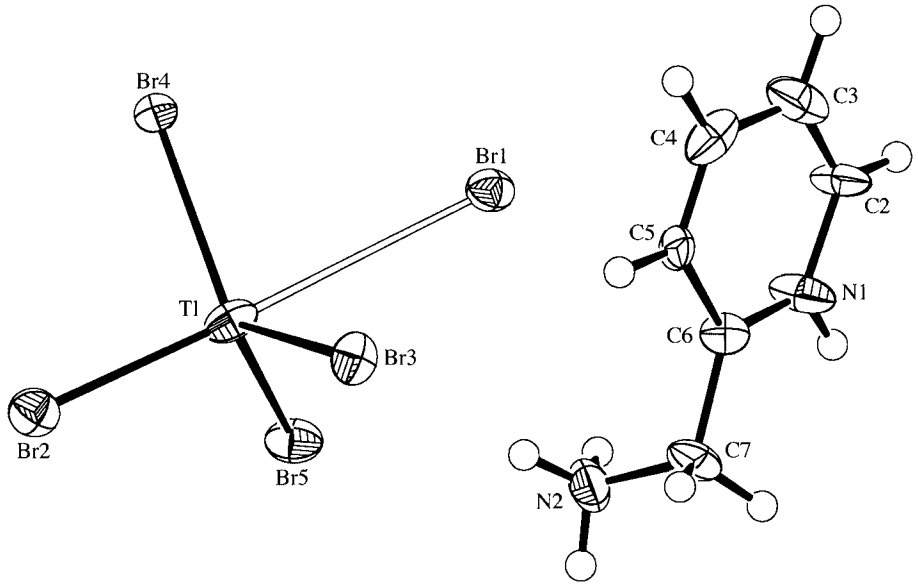

Fig. 3. *The asymmetric unit of the* $[C_6H_{10}N_2]\cdot[TlBr_5]$ (**3**) *salt highlighting the long axial Tl–Br bond* (50% probability ellipsoids)

H-bonds. In total, each cation forms H-bonds with three different anions. The combination of all interactions links the ions into infinite one-dimensional complex zig-zag chains that run parallel to the *y*-axis (*Table 4*).

Complex **3** extends the number of examples of the $[TlBr_5]^{2-}$ anion being highly distorted when it is involved in H-bonding with the cation, particularly when these interactions are predominantly with a single Br-atom, which then becomes more weakly bound to the Tl-atom. These very weak Tl ··· Br interactions, or even structures with essentially discrete $[TlBr_4]^-$ and Br^- ions, such as those of complexes **1** and **2**, seem to manifest themselves consistently in the presence of cations with N–H H-bond donors, whereas the much more regular $[TlBr_5]^{2-}$ anions are obtained in the presence quaternary ammonium cations, which, by their nature, preclude H-bonding [1].

It is interesting that the *Raman* spectrum of compound **3** (*Table 5*) corresponds to the spectra of the known $[TlBr_5]^{2-}$ entities [1][11]. It is comprised of bands that represent the three stretching modes expected for trigonal bipyramidal symmetry, as opposed to the two-stretching-mode pattern expected for tetrahedral species.

3.5. *2-Amino-4-methylpyridinium Tetrabromothallate(III)* (**4**). The asymmetric unit in the structure of complex **4** contains one cation and one $[TlBr_4]^-$ anion with neither of these entities possessing any crystallographic symmetry. The geometry of the anion is that of a very regular, undistorted tetrahedron (*Table 3*), and the shortest interionic Tl ··· Br distances, Tl ··· Br(3′) and Tl ··· Br(4″), are 4.269(1) and 4.304(1) Å, respectively. These features clearly indicate that there are no long-range interactions between the discrete $[TlBr_4]^-$ anions. The observed Tl–Br bond lengths in **3** are in agreement with those (2.2554(3) Å) found in the corresponding anion in $KTlBr_4$ [35].

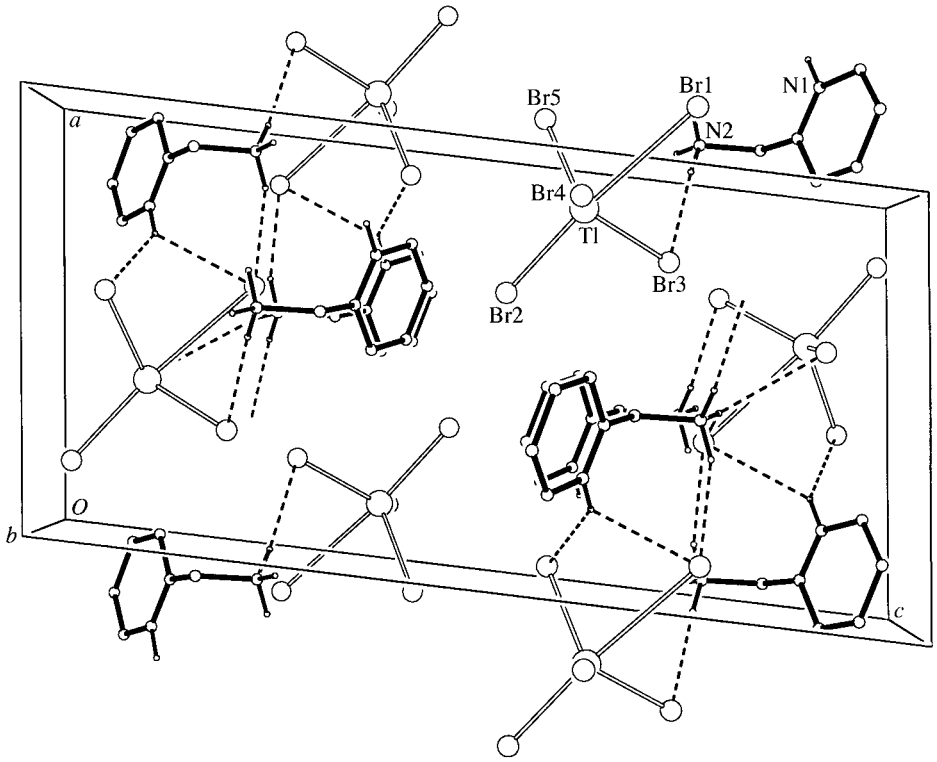

Fig. 4. *Crystal packing of* $[C_6H_{10}N_2]\cdot[TlBr_5]$ (**3**) *projected down the* b-*axis showing the H-bonding interactions as dashed lines* (uninvolved H-atoms omitted for clarity)

Table 5. Raman *Stretching Frequencies* [cm^{-1}] *for the Bromothallate(III) Complexes*

$CsTlBr_4$[a])	**1**	**2**	**4**	**5**	**6**	**7**	**8**	**9**[b])	Piperazinium $[TlBr_5]$[c])	**3**
									215.4	206
201 ν_3	196	221	209	207	211	206	210	208.2	202.7	197
184 ν_1	184	188	186	185	185	185	186	182.7	183.2	181
69 ν_4									74.1	
58 ν_2									56.2	
									35.8	

[a]) Stretching frequencies and assignments taken from [34]. [b]) Obtained on the solids by means of a *Dilor XY* confocal microprobe instrument; 614.3 nm line. [c]) Stretching frequencies and assignments taken from [11].

The cation forms a series of fairly weak H-bonds with three different surrounding anions (*Table 4*). Each of the three available N–H donors is involved in at least one interaction, with the pyridinium and one amino H-atoms forming bifurcated H-bonds. All of the Br-atoms of the $[TlBr_4]^-$ anion are involved as acceptors with one Br-atom accepting two H-bonds. These H-bonding interactions link the cations and anions into infinite two-dimensional networks that lie parallel to the (010) plane (*Fig. 5*).

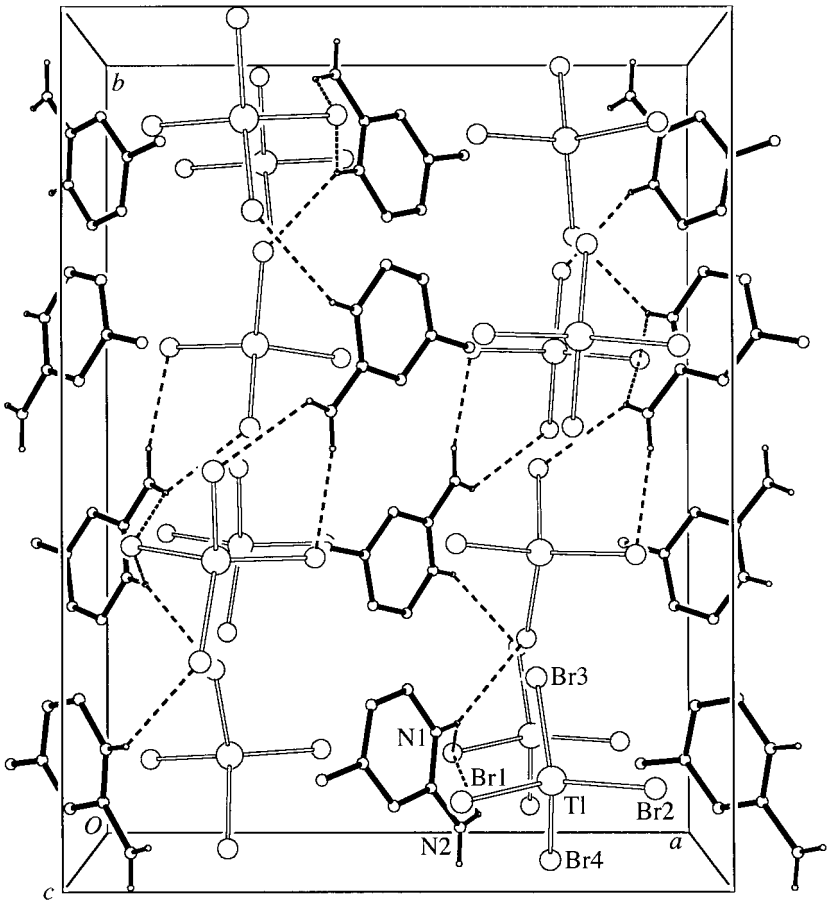

Fig. 5. *Crystal packing of* $[C_6H_9N_2] \cdot [TlBr_4]$ (**4**) *projected down the* c*-axis showing the H-bonding interactions as dashed lines* (uninvolved H-atoms omitted for clarity)

3.6. *Complexes Involving Other Pyridinium-Related Cations* (**5**–**9**). The combination of microanalytical and *Raman*-spectroscopic measurements conducted on the remaining solid-state mono- and disubstituted pyridinium bromothallate(III) salts, **5**–**9**, established that the structures all contained tetrabromothallate(III) ions, and these complexes have the $[BaseH]^+ \cdot [TlBr_4]^-$ stoichiometry (*Table 1*). The Tl–Br stretching frequencies observed for these complexes (*Table 5*) are very similar to those obtained for salts known to possess the tetrahedral $[TlBr_4]^-$ species [10][11][34]. Since the *Raman* spectra showed clearly that these complexes contained undistorted $[TlBr_4]^-$ anions, further analyses by means of X-ray crystallographic studies were not undertaken.

4. Conclusions. – In the present investigation, the employed flat mono- and disubstituted pyridinium cations did not yield any example of a complex containing a

discrete $[Tl_2Br_9]^{3-}$ anion or any other bromo-bridged system. The various pK_a values of the cations employed did not seem to have any predicatable influence on the H-bonding in this regard. Instead, the cations induce the formation of mononuclear Tl^{III} complexes that display variations on the known four- and five-coordination at the Tl-atom. Other mono- and disubstituted pyridinium derivatives having substituents other than NH_2, Me, and Br on the pyridinium ring may have inductive and resonance effects that influence the basicity of the substituted pyridine ring differently, and this, in turn, might modify the H-bonding potential of the cation and yield bromo-bridged Tl^{III} species, or a range of '$TlBr_5$' species between the $[TlBr_5]^{2-}$ and the $[TlBr_4]^-$ extremes. In this context, however, it is clear that the frequently quoted binuclear $[Tl_2Cl_9]^{3-}$ anion is a rarity (found only in the Cs salt [2][12]), and examples of chloro-bridged thallium(III) anions with organic counteractions are also uncommon [3][6][14]. Since even $Cs_3Tl_2Br_9$ does not contain the $[Tl_2Br_9]^{3-}$ anion, examples of bromo-bridging may prove to be even rarer than analogous behavior in the chlorothallate(III) systems, there being only two known occurrences so far [1][15].

An alternative strategy that might induce the formation of bromo-bridged species, for example, would be to completely eliminate the possibility of H-bonding in the pyridinium systems by employing quaternized cations and their substituted derivatives.

Also, the $Cs_3Tl_2Br_9$ salt has been found to undergo a temperature-related phase change, and the anionic structures in each phase are quite different [15]. Consequently, thermoanalytical methods might elicit whether analogous phase changes occur in recognized mixed salts such as the 1,1,3,3-tetramethylimidazolidinium derivative [10]. As the factors that govern a particular bromothallate(III) structure and stereochemistry are still being elucidated, investigations regarding these systems are ongoing.

Continued support from the Faculty of Science, Technology and Engineering, La Trobe University, is gratefully acknowledged (*B. D. J.*, *A. P.*).

REFERENCES

[1] A. Linden, A. Petridis, B. D. James, *Inorg. Chim. Acta* **2002**, *332*, 61.
[2] A. G. Lee, 'The Chemistry of Thallium', Elsevier, Amsterdam, 1971, Chapt. 3.
[3] M. A. James, J. A. C. Clyburne, A. Linden, B. D. James, J. Liesegang, V. Zuzich, *Can. J. Chem*. **1996**, *74*, 1490.
[4] M. A. James, M. B. Millikan, B. D. James, *Main Group Metal Chem*. **1991**, *14*, 1.
[5] G. Thiele, H. W. Rotter, M. Faller, *Z. Anorg. Allgem. Chem*. **1984**, *508*, 129.
[6] B. D. James, M. B. Millikan, B. W. Skelton, A. H. White, *Main Group Metal Chem*. **1993**, *16*, 335.
[7] G. Thiele, R. Richter, *Z. Kristallogr*. **1993**, *205*, 131.
[8] B. D. James, M. B. Millikan, M. F. Mackay, *Inorg. Chim. Acta* **1983**, *77*, L251.
[9] G. Thiele, B. Grunwald, *Z. Anorg. Allgem. Chem*. **1983**, *498*, 105.
[10] A. Linden, K. W. Nugent, A. Petridis, B. D. James, *Inorg. Chim. Acta* **1999**, *285*, 122.
[11] A. Linden, M. A. James, M. B. Millikan, L. M. Kivlighon, A. Petridis, B. D. James, *Inorg. Chim. Acta* **1999**, *284*, 215.
[12] A. F. Wells, 'Structural Inorganic Chemistry', 5th edn., Claredon Press, Oxford, 1984, p. 465.
[13] M. T. Kovsarnechan, J. Roziere and D. Mascherpa-Corral, *J. Inorg. Nucl. Chem*. **1978**, *40*, 2009.
[14] G. Thiele, H. W. Rotter, M. Faller, *Z. Anorg. Allgem. Chem*. **1984**, *508*, 129.
[15] K. Zimmerman, G. Thiele, *Z. Naturforsch*. *B* **1987**, *42*, 818.
[16] D. D. Perrin, 'Dissociation Constants of Organic Bases in Aqueous Solution', Butterworths, London, 1965.
[17] G. Brauer, ' Handbook of Preparative Inorganic Chemistry', 2nd edn., Academic Press, New York, 1963, Vol. 1, p. 874.

[18] P. Coppens, L. Leiserowitz, D. Rabinovich, *Acta Crystallogr.* **1965**, *18*, 1035.
[19] J. De Meulenaer, H. Tompa, *Acta Crystallogr*. **1965**, *19*, 1014.
[20] R. H. Blessing, *Acta Crystallogr., Sect A* **1995**, *51*, 33.
[21] A. Altomare, G. Cascarano, C. Giacovazzo, A. Guagliardi, M. C. Burla, G. Polidori, M. Camalli, SIR92, *J. Appl. Crystallogr.* **1994**, *27*, 435.
[22] E. N. Maslen, A. G. Fox, M. A. O'Keefe, in 'International Tables for Crystallography', Ed. A. J. C. Wilson, Kluwer Academic Publishers, Dordrecht, 1992, Vol. C, Table 6.1.1.1, pp. 477 – 486.
[23] R. F. Stewart, E. R. Davidson, W. T. Simpson, *J. Chem. Phys.* **1965**, *42*, 3175.
[24] D. C. Creagh, J. H. Hubbell, in 'International Tables for Crystallography', Ed. A. J. C. Wilson, Kluwer Academic Publishers, Dordrecht, 1992, Vol. C, Table 4.2.4.3, pp. 200 – 206.
[25] G. M. Sheldrick, SHELXL97, Program for the Refinement of Crystal Structures, University of Göttingen, Germany, 1997.
[26] M. N. Burnett, C. K. Johnson, ORTEPIII, Report ORNL-6895, Oak Ridge National Laboratory, Oak Ridge, Tennessee, USA, 1996.
[27] A. L. Spek, PLATON, Program for the Analysis of Molecular Geometry, University of Utrecht, The Netherlands, 2002.
[28] CAChe MOPAC Guide, Version 3.9 for the CAChe Work System, Oxford Molecular Group, Beaverton, Oregon, USA, 1996, p. 16.
[29] J. A. Zora, K. R. Seddon, P. B. Hitchcock, C. B. Lowe, D. P. Shum, R. L. Carlin, *Inorg. Chem*. **1990**, *29*, 3302.
[30] Z.-T. Jiang, B. D. James, J. Liesegang, C. S. Day, *Phys. Status Solidi A* **1994**, *144*, 251.
[31] Z.-T. Jiang, J. Liesegang, B. D. James, B. W. Skelton, A. H. White, *J. Phys. Chem. Solids* **1996**, *57*, 397.
[32] A. Linden, A. Petridis, B. D. James, *Acta Crystallogr.*, *Sect. C* **2002**, *58*, *m*53.
[33] N. W. Alcock, *Adv. Inorg. Chem. Radiochem*. **1972**, *15*, 1.
[34] T. G. Spiro, *Inorg. Chem*. **1967**, *6*, 569.
[35] J. Glaser, G. Johansson, *Acta Chem. Scand.*, *Ser. A* **1982**, *36*, 125.

Received October 25, 2002